J. Automation & Systems Engineering 11-2 (2017): 141-151

Regular paper

Power Control of DFIG Driven by Matrix Converter Under Super and Sub Synchronous Operation Modes

K. Bedoud, T. BAHI and H. Merabet

[1] Research Center in Industriel Technologies (CRTI) P.O. Box 64 Cheraga, Algeria.
[2] Automatic Laboratory and Signals Badji Mokhtar University, Annaba, Algeria.

JASE
Journal of Automation & Systems Engineering

Abstract- In this paper, we present the modeling and control of the wind energy conversion systems based on the doubly fed induction generator fed by AC/AC matrix converter. Firstly, we developed the models of the different elements of the conversion chain. After, we consider the vector control strategy of the active and reactive powers in order to ensure an optimum operation. Finally, the dynamic model of a doubly fed induction generator and wind turbine grid connected system is determined in the d-q synchronous reference frame.Therefore, the powers control is verified using software Matlab/Simulink. The behaviours of the sub-synchronous and super-synchronous operation modes is presented and discussed. The results prove that the power control strategy is well adapted to this kind of system.

Keywords: Wind Systems, Doubly Fed Induction Generator, Bidirectional DC-DC Converter, Variable Speed Wind Turbine.

1. INTRODUCTION

Renewable energy is an inexhaustible, clean and efficient energy source. Wind energy has become the most used source of energy due to its many quality such as: while producing electricity they do not propagate any gas green house effect, do not degrade the quality of the air and do not pollute nor the soils or waters and it do not produce toxic or radioactive waste [1, 2].The operation of a wind turbine at variable speed is more beneficial over constant speed operation. A variable speed generator based wind turbine allows extracting maximum power from the wind than a fixed speed wind turbine. Nowadays, wind generation system based on a doubly fed induction generator (DFIG) are widely employed in large wind farms fat has its many advantages [2-6].The conventional wind energy conversion systems (WECS) is constituted of the turbine, the gearbox and the DFIG. The DFIG is connected directly to the grid via its stator but also via its rotor by means of two static converters to allow an exchange of energy between the network and the DFIG at the speed of synchronism. The rotor-side converter (RSC) and the grid-side converter (GSC) are connected back-to-back by a dc-link capacitor [7]. So, for remedy the use of two converters and to reduce maintenance, cost and number of components. The three phase matrix converter (MC) can be used for a direct AC/AC conversion without dc-link connection [8-10].The MC is widely employed in large wind farms that have many advantages: direct power converter AC/AC, bi-directional power flow, nearly sinusoidal input and output waveform, and allows to control: the rotor currents magnitude, frequency and input power factor [9-11]. The aim of this work is to prove the decoupling powers control of wind energy conversion system driven by matrix converter under hypo and hyper-synchronous operation modes.

The paper is organized as follows. Section 2, presents the description and the modeling of different elements of the conversion chain. The control strategy will be presented in section 3. The results of simulations obtained for the two modes sub-synchronous and super-synchronous modes will be exposed and discussed in Section 4. Finally, the conclusions are established.

2. WIND TURBINE SYSTEM MODELING

In this work, we consider the configuration presented by Fig1. It is constituted mainly of: an aero-turbine, gearbox and the DFIG. The DFIG is directly connected to the grid via its stator but also via its rotor by means of three-phase matrix converter. The matrix converter provides bi-directional power flow, which permits to the DFIG to work in sub-synchronous and super-synchronous operation modes.

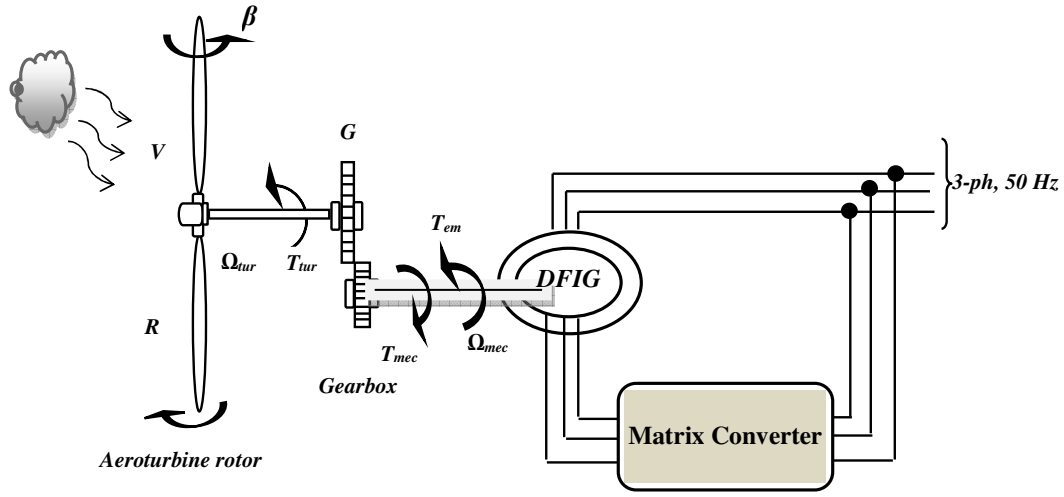

Fig. 1. Schematic diagram of DFIG wind turbine fed by MC

2.1 Turbine Modeling

The theoretical power produced by the wind is given by [12]:

$$P_{tur} = C_p.\frac{\rho.S.V^3}{2} \quad (1)$$

Where C_p denotes power coefficient of wind turbine, its evolution depends on the blade pitch angle (β) and the tip-speed ratio (λ) which is defined as [13]:

$$\lambda = \frac{R.\Omega_{tur}}{V} \quad (2)$$

ρ, V and R are the air density, wind speed and rotor radius, respectively. From summaries achieved on a wind of 1.5 MW, the expression of the power coefficient for this type of turbine can be approximated by the following equation [1, 7]:

$$C_p = \left(0.45 - \left(0.0167(\beta - 2)\right)\right)\left(sin\left(\frac{\pi(\lambda+0.1)}{\left(15.5-\left(0.3(\beta-2)\right)\right)}\right)\right) - \left(0.00184(\lambda - 3)(\beta - 2)\right) \quad (3)$$

The aerodynamic torque expression is given by [13]:

$$T_{tur} = \frac{P_{tur}}{\Omega_{tur}} = C_p.\frac{\rho.S.V^3}{2}.\frac{1}{\Omega_{tur}} \quad (4)$$

The gearbox is installed between the turbine and the generator to adapt the turbine speed (Ω_{tur}) to that of the generator (Ω_m), with G is gearbox ratio:

$$\Omega_{mec} = G.\Omega_{tur} \tag{5}$$

The friction, elasticity and energy losses in the gearbox are neglected.

$$G = \frac{T_{tur}}{T_{mec}} \tag{6}$$

The mechanical equations of the system can be characterized by:

$$J\frac{d\Omega_{mec}}{dt} = T_{mec} - T_{em} - f\Omega_{mec} \tag{7}$$

With, $J = \frac{J_{tur}}{G^2} + J_{gen}$

J : turbine total inertia;
f : friction coefficient.

2.2 Modeling of the DFIG with stator field orientation

The model of DFIG is given by the equations below:

$$\begin{bmatrix} V_{as} \\ V_{bs} \\ V_{cs} \end{bmatrix} = \begin{bmatrix} R_s & 0 & 0 \\ 0 & R_s & 0 \\ 0 & 0 & R_s \end{bmatrix} \begin{bmatrix} i_{as} \\ i_{bs} \\ i_{cs} \end{bmatrix} + \frac{d}{dt} \begin{bmatrix} \varphi_{as} \\ \varphi_{bs} \\ \varphi_{cs} \end{bmatrix} \tag{8}$$

$$\begin{bmatrix} V_{ar} \\ V_{br} \\ V_{cr} \end{bmatrix} = \begin{bmatrix} R_r & 0 & 0 \\ 0 & R_r & 0 \\ 0 & 0 & R_r \end{bmatrix} \begin{bmatrix} i_{ar} \\ i_{br} \\ i_{cr} \end{bmatrix} + \frac{d}{dt} \begin{bmatrix} \varphi_{ar} \\ \varphi_{br} \\ \varphi_{cr} \end{bmatrix} \tag{9}$$

The stator and rotor flux as a function of currents are given as:

$$\begin{bmatrix} \varphi_{as} \\ \varphi_{bs} \\ \varphi_{cs} \end{bmatrix} = \begin{bmatrix} L_s & M_s & M_s \\ M_s & L_s & M_s \\ M_s & M_s & L_s \end{bmatrix} \begin{bmatrix} i_{as} \\ i_{bs} \\ i_{cs} \end{bmatrix} + [M_{sr}] \begin{bmatrix} i_{ar} \\ i_{br} \\ i_{cr} \end{bmatrix} \tag{10}$$

$$\begin{bmatrix} \varphi_{ar} \\ \varphi_{br} \\ \varphi_{cr} \end{bmatrix} = \begin{bmatrix} L_r & M_r & M_r \\ M_r & L_r & M_r \\ M_r & M_r & L_r \end{bmatrix} \begin{bmatrix} i_{ar} \\ i_{br} \\ i_{cr} \end{bmatrix} + [M_{sr}] \begin{bmatrix} i_{as} \\ i_{bs} \\ i_{cs} \end{bmatrix} \tag{11}$$

Where quantities with subscript s or r denote stator or rotor quantities. The voltage and currents vectors are, respectively,$[V_{as} \quad V_{bs} \quad V_{cs}]^T$, $[V_{ar} \quad V_{br} \quad V_{cr}]^T$ and $[I_{ar} \quad I_{br} \quad I_{cr}]^T$, $[I_{as} \quad I_{bs} \quad I_{cs}]^T$. φ denotes flux linkage, R is resistance, L_s and L_r are the stator and rotor self inductances, respectively. M_s and M_r denote, respectively, the mutuel-inductances between stator and rotor phases. The mutual inductances matrix ($[M_{sr}]$) depends on the angular position (θ) between stator and rotor axis.

$$[M_{sr}] = [M_0] \begin{bmatrix} cos\theta & \cos(\theta - \frac{4\pi}{3}) & \cos(\theta - \frac{2\pi}{3}) \\ \cos(\theta - \frac{2\pi}{3}) & cos\theta & \cos(\theta - \frac{4\pi}{3}) \\ \cos(\theta - \frac{4\pi}{3}) & \cos(\theta - \frac{2\pi}{3}) & cos\theta \end{bmatrix} \tag{12}$$

With M_0 is the maximum of the mutual inductance between a stator phase and the corresponding rotor phase.

Consider that the load torque (T_r) is a disturbing input, the modelization of DFIG expressed in a (d-q) synchronous rotating frame is presented by the equations below :

$$\frac{d}{dt}\begin{bmatrix} i_{sd} \\ i_{sq} \\ i_{rd} \\ i_{rq} \\ \omega \\ \theta \end{bmatrix} = \begin{bmatrix} -a_1 i_{sd} + (a\omega + \omega_s) i_{sq} + a_3 i_{rd} + a_5 \omega i_{rd} \\ -(a\omega + \omega_s) i_{sd} - a_1 i_{sq} - a_5 \omega i_{rd} + a_3 i_{rq} \\ a_4 i_{sd} - a_6 \omega i_{sq} - a_5 \omega i_{rd} + \left(\omega_s - \frac{\omega}{\sigma}\right) i_{rq} \\ -a_6 \omega i_{sd} - a_4 i_{sq} - \left(\omega_s - \frac{\omega}{\sigma}\right) i_{rd} - a_5 \omega i_{rq} \\ m_1 \left(i_{sq} i_{rd} - i_{sd} i_{rq}\right) - m_2 \\ \omega \end{bmatrix} + \begin{bmatrix} b_1 & 0 & -b_3 & 0 & 0 \\ 0 & b_1 & 0 & -b_3 & 0 \\ -b_3 & 0 & b_2 & 0 & 0 \\ 0 & -b_3 & 0 & b_2 & 0 \\ 0 & 0 & 0 & 0 & -m_3 \\ 0 & 0 & 0 & 0 & 0 \end{bmatrix} \begin{bmatrix} V_{sd} \\ V_{sq} \\ V_{rd} \\ V_{rq} \\ T_r \end{bmatrix} \tag{13}$$

Where :

$$a = \frac{1-\sigma}{\sigma}, a_1 = \frac{R_s}{\sigma L_s}, a_2 = \frac{R_r}{\sigma L_r}, a_3 = \frac{R_r M_{sr}}{\sigma L_r L_s}, a_4 = \frac{R_s M_{sr}}{\sigma L_s L_r}$$
$$a_5 = \frac{M_{sr}}{\sigma L_s}, a_6 = \frac{M_{sr}}{\sigma L_r}, b_1 = \frac{1}{\sigma L_s}, b_2 = \frac{1}{\sigma L_r}, b_3 = \frac{M_{sr}}{\sigma L_s L_r}$$
$$\sigma = 1 - \frac{M_{sr}^2}{L_s L_r}, m_1 = \frac{P^2 M_{sr}}{J}, m_2 = \frac{F}{J}, m_3 = \frac{P}{J}$$

The quantities with subscript q or d denote q axis or d axis quantities. ω_s is synchronous angular frequency. The DFIG is presented in synchronously rotating d–q axis frame with the d-axis oriented along the stator flux vector position, and then, ($\varphi_{sq} = 0, \varphi_{sd} = \varphi_s$) [1]. In this way, a decoupled control between the active and reactive powers is obtained. Furthermore, considering that the resistance of the stator winding (R_s) is neglected and the grid is supposed stable with voltage v_s and synchronous angular frequency (ω_s) constant what implies $\varphi_{sd} = cst$, the voltage and the flux equations of the stator windings can be simplified in steady state as:

$$\begin{cases} V_{sd} = \frac{d\varphi_{sd}}{dt} = 0 \\ V_{sq} = \omega_s . \varphi_{sd} = V_s \end{cases} \tag{14}$$

Stator and rotor active and reactive powers are described as [7]:

$$\begin{cases} P_s = -\frac{V_s . M}{L_s} . i_{rq} \\ Q_s = \frac{V_s^2}{L_s \omega_s} - \frac{M . V_s}{L_s} . i_{rd} \\ P_r = g . \frac{V_s . M}{L_s} . i_{rq} \\ Q_r = g . \frac{V_s . M}{L_s} . i_{rd} \end{cases} \tag{15}$$

The electromagnetic torque is as follows [7]:

$$T_{em} = -P . \frac{M}{L_s} \varphi_{sd} . i_{rq} \tag{16}$$

With, *P* is the number of poles.

2.3 Modeling of Matrix Converter

The matrix converter studied in this paper is 9×3 bidirectional switch single pole power converter. It is used to convert nine AC phase input voltage into three AC phase output, with a control of magnitude and frequency current output. The tree phase output (V_a, V_b, V_c) and input (V_A, V_B, V_C)voltages are represented in terms of input voltages by (14). In

addition, the input currents (I_A, I_B, I_C) can also be calculated in terms of output currents (I_a, I_b, I_c) using equation (18) [15, 16]:

$$\begin{bmatrix} V_a \\ V_b \\ V_c \end{bmatrix} = \begin{bmatrix} S_{Aa} & S_{Ba} & S_{Ca} \\ S_{Ab} & S_{Bb} & S_{Cb} \\ S_{Ac} & S_{Bc} & S_{Cc} \end{bmatrix} \begin{bmatrix} V_A \\ V_B \\ V_C \end{bmatrix} \tag{17}$$

$$\begin{bmatrix} I_A \\ I_B \\ I_C \end{bmatrix} = \begin{bmatrix} S_{Aa} & S_{Ab} & S_{Ac} \\ S_{Ba} & S_{Bb} & S_{Bc} \\ S_{Ca} & S_{Cb} & S_{Cc} \end{bmatrix} \begin{bmatrix} V_a \\ V_b \\ V_c \end{bmatrix} \tag{18}$$

Where the transfer matrix of MC is defined by the switching function (S_{jk}) as:

$$S_{jk} = \begin{cases} 1 \rightarrow S_{jk}\ closed \\ 0\ \rightarrow S_{jk}\ open \end{cases}, \mathrm{j}\epsilon\{A,B,C\}, k\epsilon\{a,b,c\} \tag{19}$$

Knowing that the transfer matrix of calculating input currents is the transpose of the transfer matrix in equation (15). Calculation time of each output phase voltage t_{jk} is a fraction of the switching frequency period T_s.

$$t_{jk} = S_{jk}.T_s \tag{20}$$

With, $\sum t_{ja} = \sum t_{jb} = \sum t_{jc} = T_s$

To eliminate open circuit to the output terminals or short circuit between input terminals, the switching constraint is defined as follow:

$$\sum S_{ja} = \sum S_{jb} = \sum S_{jc} = 1 \tag{21}$$

The maximum ratio between output and the input voltage is 86,6% [10].

$$q = \sqrt{\frac{V_o^2}{V_i^2}} \text{ with:} 0 < q \leq 0.866 \tag{22}$$

Based on the equations (21) and (22) matrix transfer can be calculated by the following three equations:

$$S_{jk} = \frac{1}{3} + \frac{2}{3}\frac{V_j V_k}{V_{iS}^2} + \frac{2}{9}\frac{q}{q_S}\sin\left(\omega_i t + \emptyset_j\right).\sin(3\omega_i t) \tag{23}$$

$$V_j = V_{iS}\cos(\omega_i t + \emptyset_j) \tag{24}$$

$$V_k = q\, V_{iS}\cos(\omega_0 t + \emptyset_k) - \frac{q}{6}V_{iS}\cos(3\,\omega_0 t) + \frac{1}{4}\frac{q}{q_S}V_{iS}\cos(3\omega_i t) \tag{25}$$

The Simulink bloc diagram of MC developed in this work is showing in Fig.2.

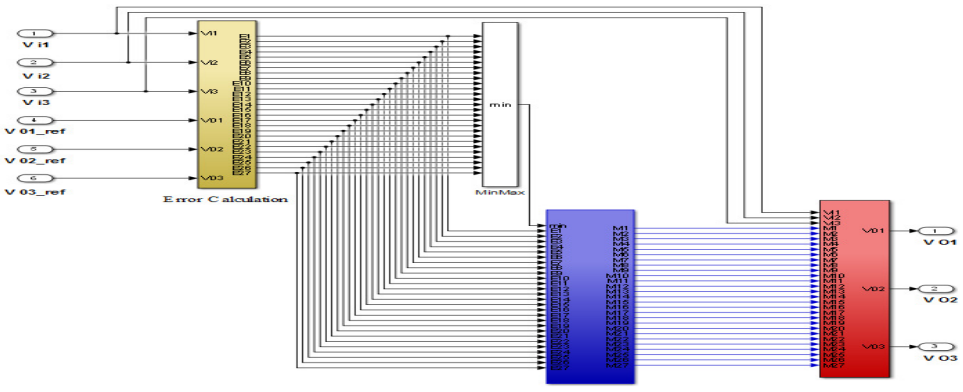

Fig. 2. Circuit diagram of MC

3. CONTROL STRATEGY

Preliminary work [6, 17] has shown the performance of the system using converters connected back-to-back by DC bus. However, this control structure despite its good performances, presents a certain inconvenience number and imperfection in the control. Especially, three step power conversion AC-DC-AC, complex structure and also high cost and important number of components. Based on these remarks, the interest of this paper is to propose another control configuration based on a MC and to improve decoupling powers control of WECS driven by matrix converter under hypo and hyper-synchronous operation modes. The studied system is shown in Fig.3. The modulation method (LMSE) is used to control the MC. The operation of a wind turbine at variable speed is generally more beneficial over constant speed operation [7]. In this section two control loops are presented: control loop of the electric generator via matrix converter and control loop of the aero-turbine without speed control that provides the reference inputs of the first loop. The extraction of maximum power control is to adjust the torque of the DFIG to extract maximum power. In effect, the power extracted from the wind is maximized when the rotor speed is such that the power coefficient is optimal C_{popt}. Therefore, we must set the tip speed ratio on its optimal value λ_{opt}. Tab. 1 recapitulates the variation of the optimal power coefficient (C_{popt}) versus the tip-speed ratio (λ_{opt}) for the different values of pitch angle (β).So, we can notice that there is one specific point (λ_{opt}, C_{popt}) at which the turbine is most efficient.

Tab. 1 Power coefficient versus tip speed ratio and pitch angle

λ_{opt} β(°)	**7.5**	**7.8**	**7.06**	**7.14**
2	0.45	0.44	0.44	0.44
3	0.42	0.43	0.42	0.42
4	0.39	0.39	0.4	0.4
5	0.37	0.37	0.37	0.38

In the next part of this study, we opted for β=2°. For it, we have λ_{opt} andC_{popt}, respectively, equal to 7.5 and 0.45. The electromagnetic torque reference determined by MPP control power is thus expressed by the following equation [17, 18]:

$$T_{em}^{*} = \frac{C_{popt}.\rho.\pi.R^5}{2.G^3.\lambda_{opt}^3}.\Omega_m^2 \tag{26}$$

Equation (15) and (16) demonstrate that the electromagnetic torque and the stator reactive power can be controlled by means of the DFIG current i_{rq} and i_{rd} respectively. The model of DFIG in d-q reference frame with stator field orientation shows that the rotor currents can be controlled independently. The reference rotor currents i_{rd_ref} and i_{rq_ref} are given by:

$$i_{rd\_ref} = \frac{\varphi_{sd}}{M} - \frac{L_S}{M.V_{Sq}}.Q_{s\_ref} \tag{27}$$

$$i_{rq\_ref} = -\frac{L_S}{M.P.\varphi_{sd}}.T_{em}^{*} \tag{28}$$

The proportional integral controller (PI) is widely used in the control of DFIG because of its simple structures and good performances. For the synthesis of the regulators we opted for the method of poles compensation (t_r= 0.005s).

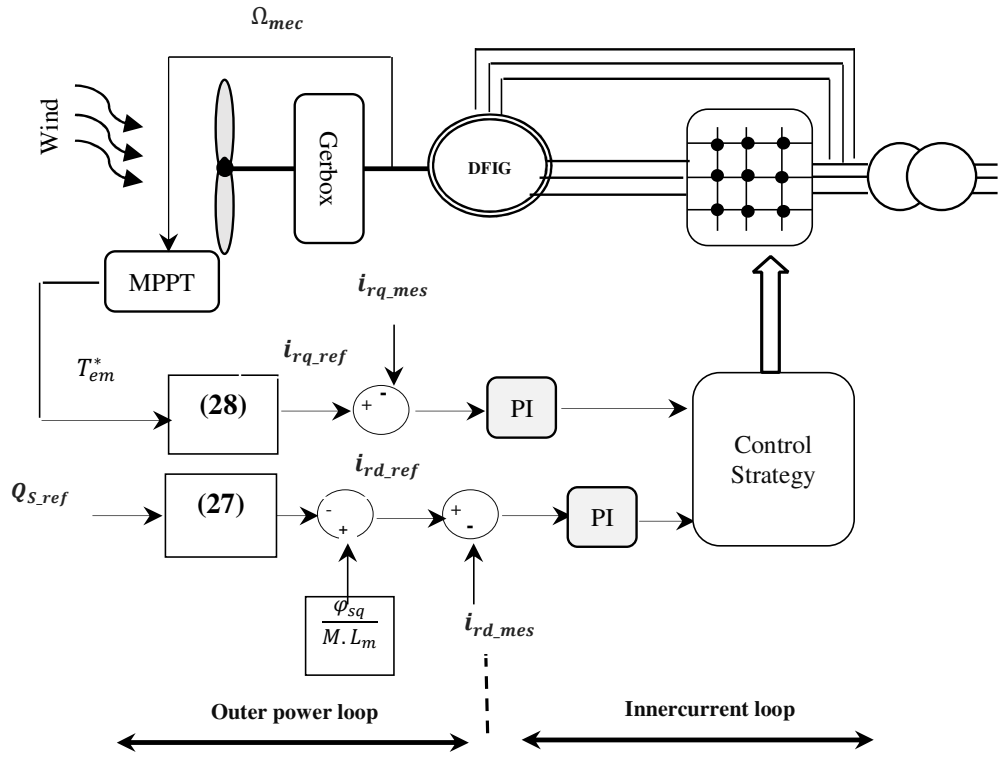

Fig. 3. Circuit diagram of WECS with MC

4. SIMULATION RESULTS

In order to analyze the performances under the different operation modes of the structure studied, we have considered the profiles of the active (P_s) and reactive (Q_s) powers references are summarized in table 2.

Tab. 2 Operation Statues of the Simulated DFIG

Time (s)	P (MVar)	Time (s)	Q (MW)
0 ≤ t≤0.15	-0.5	0 ≤t ≤0.25	0.5
0.15< t≤0.4	0	0.25< t ≤0.6	-0.2
0.4< t≤0.75	-0.3	0.6< t ≤0.9	0.7
0.75< t ≤1	0.9	0.9< t ≤1.2	0
1< t ≤1.2	0.3		-

The studied system has been tested in sub-synchronous and super-synchronous modes. The Figures 4, 6 and Figures 5, 7 show the simulation results corresponding, respectively, sub-synchronous and super-synchronous modes. For this, the unity power factor in the connection of the matrix converter with the grid is obtained by setting $Q_{s-ref} = 0$.
The speed wind 7m/s and 13m/s correspond 1490rd/min and 2340rd/min at the machine speed (Fig.8a and Fig.8-b).

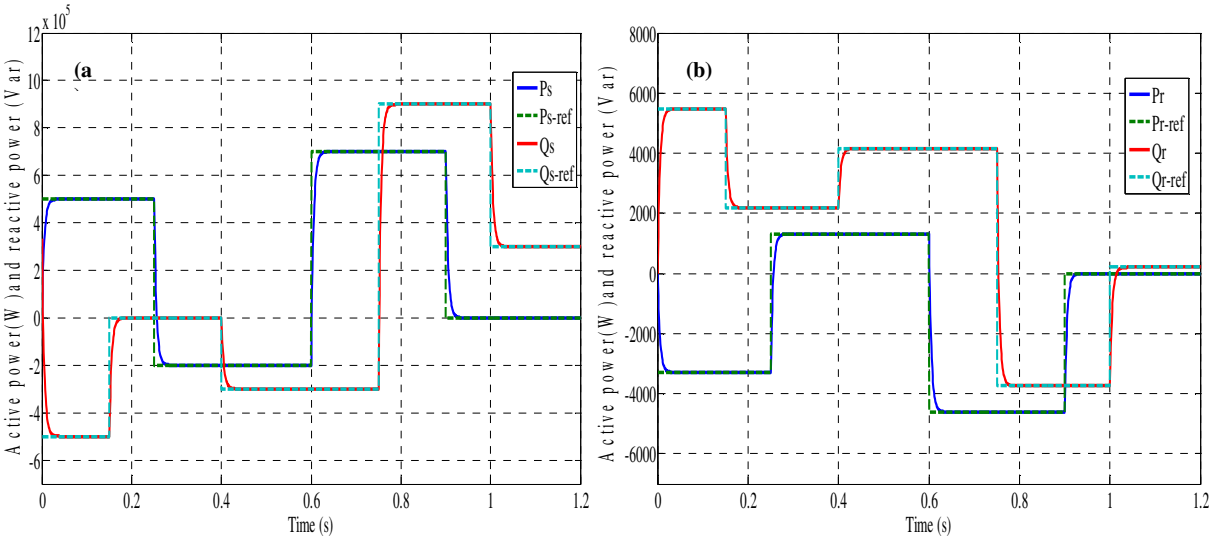

Fig. 4. Active and reactive powers (a)-stator (b)-rotor under sub-synchronous mode

Figures 4-a and 4-b, shows, respectively, the forms of the active and reactive powers under sub-synchronous mode. Concerning the time interval (0-0.3s), we first change Q_s at time t=0.15s and then P_s at time t=0.25sas shown in the Figures 4a and 5a. We remark that the change of one of these size do not influence the change of the other, which testifies a decoupled control of the active and reactive power, both in sub-synchronous mode (Fig.4. a) and super-synchronous (Fig.5.a).

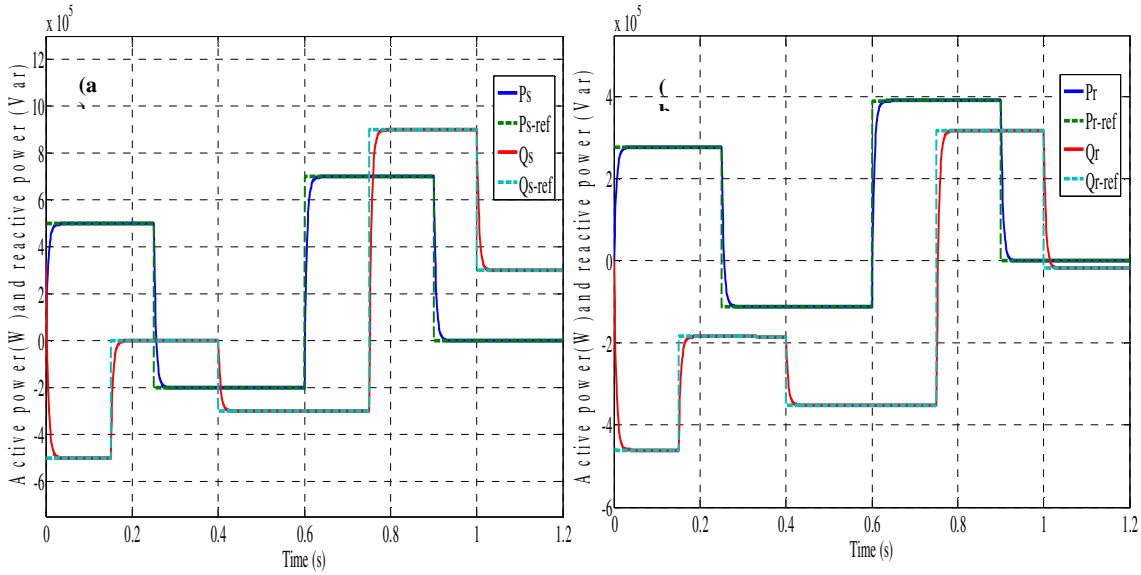

Fig. 5. Active and reactive powers (a)-stator (b)-rotor under super- synchronous mode

Note that for the time interval (0.15-0.4s), we held to show the functioning of the wind system with a unity power factor (Q_{s-ref}= 0). However, allow for the functioning of the DFIG in the different quadrants, during the time interval (0.4-0.8s), we changed P_{s-ref} and Q_{s-ref}in the opposite sense of the previous interval. It is found that the control remain decoupled.

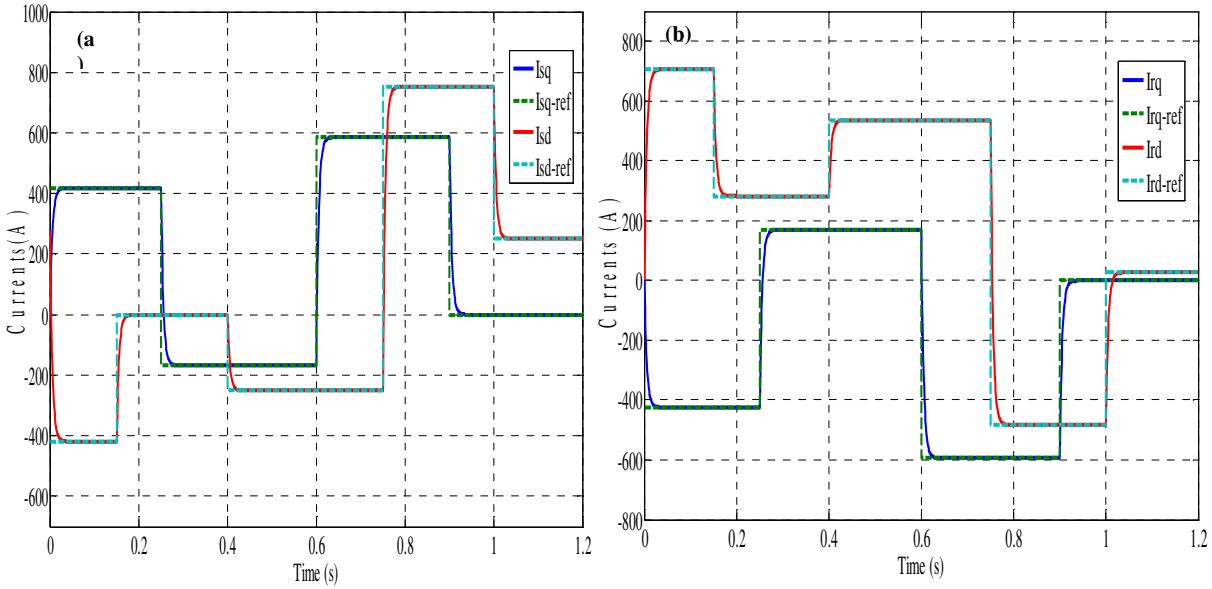

Fig. 6. (a)-stator (b)-rotor currents under sub- synchronous mode

Finally, during (0.9-1.5s), only Qs is changed while keeping P_s constant. Under these operating conditions, we remark that the power active and reactive to the rotor (see Fig.4.b and Fig.5.b) evolve correctly.

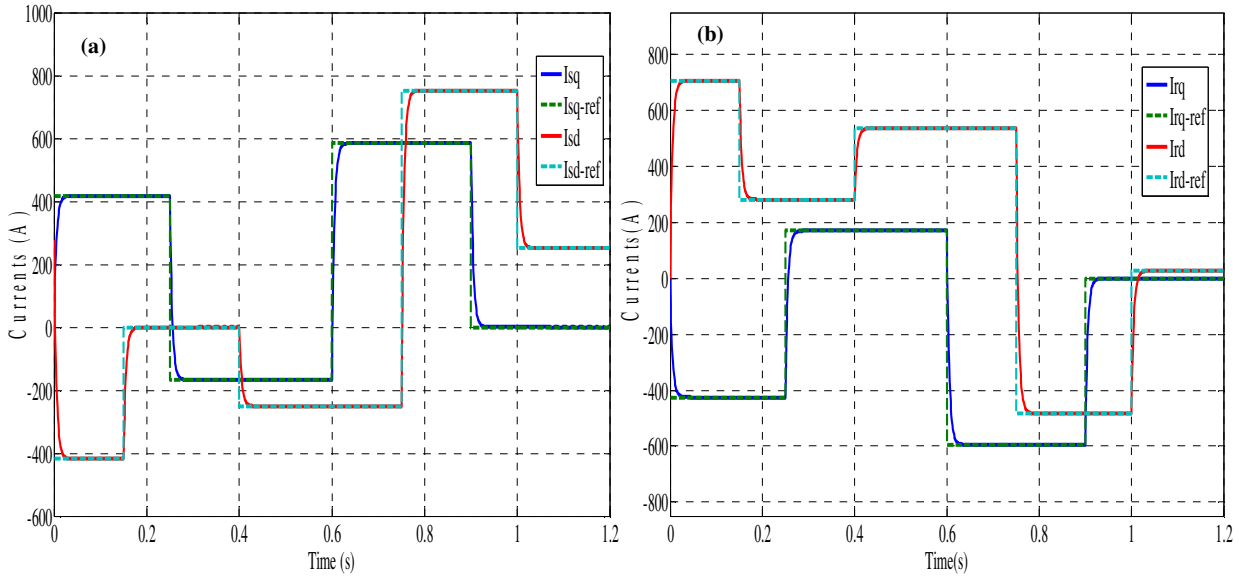

Fig. 7. (a)-Stator (b)-Rotor currents under super- synchronous mode

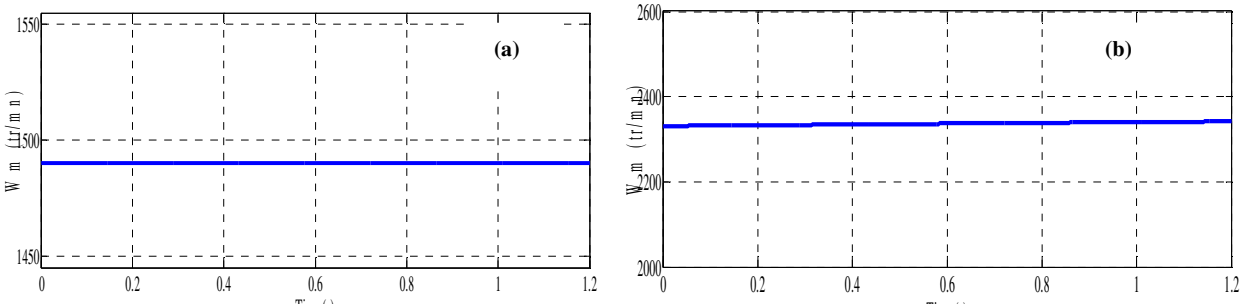

Fig. 8. Speed machine : (a)-sub-synchronous ,(b)-super-synchronous

However, we notice that since the DFIG needs a reactive power necessary to its magnetization and as the stator reactive power is null ($Q_s = 0$), the DFIG absorbs the reactive power by the rotor. Figures 6 and 7 show the evolution of the stator, rotor currents in sub-synchronous and super-synchronous mode, respectively.

The currents normally follow the evolutions of the powers previously discussed for the case of stator currents Fig.6a and Fig.7a, whereas the currents to the rotor Fig.6b and Fig.7 be volve identically to the rotor active power in sub-synchronous mode and inversely in super-synchronous mode. In effect, there is a perfect decoupling between the two power components. Indeed, despite the change in the references of reactive powers and consequently of their corresponding magnitudes, the active power keep a value corresponding to the maximum of the developed power.

5. CONCLUSION

This paper exposes the powers control strategy of wind energy conversion system based on doubly fed induction generator driven by matrix converter, which provides decoupled control of active and reactive power. However, the fact of the control of these powers separately permits to adjust the power factor of the installation and in consequence obtain better performance. Therefore, the detailed modeling of the mechanical part of the wind turbine taking into account the characteristics of the blade profile used and the wedging angle, and the mechanical assembly includes the gearbox is presented. Also, a good stabilization of the active powers is noted even if the reactive power varies. The simulation results using software Matlab/Simulink show that the use of matrix converter has given us good rotor currents and power waveforms and can operate with a unit power factor. Finely, we not that, the simulation results show that the stator active and reactive control powers, give a good performance. Hence, the power control strategy is well adapted to this kind of system.

REFERENCES

[1] K. Bedoud , T. Bahi , H. Merabet , Comparative Study of Wind Energy Conversion System Driven by Matrix Converter and AC/DC/AC Converter, Proceedings of the International Conference on Recent Advances in Electrical Systems , Vol. 1 , Issue 1, pp 301-306, 2016.

[2] R. Cardenas, R. Pena, J. Proboste, G. Asher and J. Clare. “MRAS observer for sensorless control of standalone doubly fed induction generators,” IEEE Transaction on Energy Convertion, Vol. 20, pp. 710–718, 2005.

[3] S. Karimi, A. Gaillard,P. Poure,S. Saadate, FPGA-Based Real-Time Power Converter Failure Diagnosis for Wind Energy Conversion Systems, IEEE Transactions on Industrial Electronics, Vol. 55, N. 12, 2008.

[4] Tazil M, Kumar V, Bansal RC, Kong S, Dong ZY, Freitas W, MathurHD, “Three-phase doubly fed induction generators: an overview,” IET Electric Power Applications, Vol. 4, pp. 75-89, 2010.

[5] O. Anaya-Lara, N. Jenkins, J. Ekanayake,P. Cartwright,M. Hughes, Wind energy generation: Modelling and control. Chichester, UK: John Wiley & Sons, 2009.

[6] E. Tremblay, S. Atayde, A.Chandra, Direct Power Control of a DFIG-based WECS with Active Filter Capabilities, IEEE Electrical Power & Energy Conference, 2009.

[7] K. Bedoud and all, "Robust Control of Doubly Fed Induction Generator for Wind Turbine Under Sub-Synchronous Operation Mode," Energy Procedia, Vol. 74n pp. 886 – 899, 2015.

[8] SKM. Ahmed, A. Iqbal.,H. Abu-Rub, J. Rodriguez, C. Rojas, "Simple carrier-based PWM technique for a three to nine phase matrix converter," IEEE Trans. On Ind. Elect., Vol. 58, no. 11, pp. 5014-5023, Nov.2011.

[9] O. Abdel-Rahim, H. Abu-Rub, A. Kouzou, "Nine-to-Three Phase Direct Matrix Converter with ModelPredictive Control for Wind Generation System," Energy Procedia, Vol.42, pp. 173 – 182, 2013.

[10] B. Hamane, M. L. Doumbia, M. Bouhamida, H. Chaoui, M. Benghanem, "Modeling and Control of a Wind Energy Conversion System Based on DFIG Driven by a Matrix Converter," IEEE Eleventh International Conference on Ecological Vehicles and Renewable Energies (EVER), 2016.

[11] V. Vasipalli, S. P. Phulambrikar, A. Agrawal, "Power Quality Improvement in DFIG System with Matrix Converter in Wind Energy Generation with Space Vector Control Techniques," IEEE Inter. Conf. Technological Advancements in Power & Energy, 2015.

[12] O. Barambones, Jose M. Gonzalez de Durana, E. Kremers, Adaptive robust control to maximizing the power generation of a variable speed wind turbine, International Conference on Renewable Energy Research and Applications Madrid, Spain, 20-23 October 2013.

[13] S. Abdeddaim, A. Betka, "Optimal tracking and robust power control of the DFIG wind turbine, Electrical Power and Energy Systems," Vol.49, pp. 234-242, 2013.

[14] Ahmed M. Kassem, Khaled M. Hasaneen, Ali M. Yousef, "Dynamic modeling and robust power control of DFIG driven by wind turbine at infinite grid, Electrical Power and Energy Systems," Vol. 44, pp. 375-382, 2013.

[15] A. Huseyin, S. Sedat, Modeling, "Simulation and control of wind turbine driven doubly-fed induction generator with matrix converter on the rotor side," Elect. Eng, Vol. 95, pp. 157-170, 2013.

[16] M. Sherif, A.A. Dabour, , A. Shehab , M. Ahmed , "Performance of a Three-to-Five Matrix Converter Fed Five-Phase Induction Motor under Open-Circuit Switch Faults," Computer Applications & Industrial Electronics, IEEE Symposium, 2016.

[17] K. Bedoud, M. Ali Rachedi, R. Lakel, T. Bahi, "Adaptive Fuzzy Gain Scheduling of PI Controller for control of the Wind Energy Conversion Systems, Energy Procedia, Vol. 74, pp. 211-225, 2015.

[18] M. Boutoubat, L. Mokrani, M. Machmoum, "Control of a wind energy conversion system equipped by a DFIG for active power generation and power quality improvement," Renewable Energy, Vol. 50, pp. 378-386, 2013.